Low-energy fine-structure resonances in photoionization of O II

Sultana N. Nahar,[1,*] Maximiliano Montenegro,[2] Werner Eissner,[3] and Anil K. Pradhan[1]
[1]*Department of Astronomy, The Ohio State University, Columbus, Ohio 43210, USA*
[2]*Facultad de Educaci, Pontificia Universidad Catholica de Chile, Avda Vicua Mackenna 4860, Macul, Santiago, Chile*
[3]*Institut für Theoretische Physik, Teilinstitut 1, D-70550 Stuttgart, Germany*
(Received 12 October 2010; published 20 December 2010)

Resonant features in low-energy photoionization cross sections are reported in coupled-channel calculations for O II including relativistic fine structure. The calculations reveal extensive near-threshold resonant structures in the small energy region between the fine structure levels of the ground state $2p^2(^3P_{0,1,2})$ of the residual ion O III. Although the resonances have not yet been observed, they are similar to other experimentally observed features. They are expected to significantly enhance the very-low-temperature dielectronic recombination rates, potentially leading to the resolution of an outstanding nebular abundances anomaly. Higher energy partial and total photoionization cross sections of the ground configuration levels $2p^3(^4S^o_{3/2},^2D^o_{3/2,5/2},^2P^o_{1/2,3/2})$ are found to be in agreement with experimental measurements on synchrotron-based photon sources [1–3], thereby identifying the excited O III levels present in the ion beams. These are also the first results from a recently developed version of Breit-Pauli *R*-matrix (BPRM) codes, with inclusion of two-body magnetic interaction terms. The improved relativistic treatment could be important for other astrophysical applications and for more precise benchmarking of experimental measurements.

DOI: 10.1103/PhysRevA.82.065401 PACS number(s): 32.80.Fb, 95.30.Ky

I. INTRODUCTION

As one of the most abundant elements, the study of oxygen and its ions is of great importance in astronomy, atmospheric sciences, and laboratory devices. Singly ionized O II has been extensively studied experimentally [1–3] as well as theoretically [4,5]. Using synchrotron-based photon sources such as the Advanced Light Source (ALS) [1,3], high-resolution experimental measurements of photoionization cross sections of O II reveal a number of Rydberg series of resonances converging on various excited states of the residual ion O III. These resonances are known to significantly attenuate the cross sections and thereby the total rate in a given environment. Given the low temperatures of 1000–10 000 K where O II and O III occur, theoretical calculations need to resolve the resonances in the low-energy range just above the ionization threshold(s).

The astrophysical importance lies in the fact that there are large discrepancies in abundances of several nebular elements, including C, N, O, S, Fe, and Ni, derived from recombination lines, as opposed to collisionally excited lines [6–8]. The present study on O II is also aimed at a possible resolution of this outstanding problem. Photoionization of O II determines the abundance of O III, which is of crucial importance since its emission lines are prime diagnostics of the plasma environment. The inverse process of electron-ion recombination $(e + \text{O III}) \rightarrow \text{O II}$ gives rise to recombination lines whose intensities yield a measure of the oxygen abundance in the source. There has been a longstanding and surprising discrepancy between oxygen abundances derived from collisionally excited forbidden lines of [O III] on the one hand, and optical recombination lines on the other hand. Since the collision strengths for [O III] transitions are known accurately, it is likely that the uncertainties in low-temperature recombination rate coefficients of O II are responsible for the abundance discrepancy. At very low temperatures ~100–10 000 K, recombination via low-energy resonances (i.e., dielectronic recombination) could enhance the total electron-ion recombination rate considerably, compared to those computed previously in *LS* coupling [9]. However, ascertaining recombination rate coefficients in the very low-T regime of <1000 K depends on the accuracy of photoionization cross sections just above the ionization threshold(s). That, in turn, may be heavily enhanced by the presence of near-threshold autoionizing resonances, which therefore need to be delineated precisely.

The present work reports photoionization calculations for O II, including fine structure, and has been carried out using the relativistic Breit-Pauli *R*-matrix (BPRM) method, including higher order two-body magnetic interactions which have not been heretofore considered.

II. THEORY AND COMPUTATIONS

The coupled channel (CC) approximation using the BPRM method entails a wave function expansion $\Psi(E)$ for the $(N + 1)$ electron system, with total spin and orbital angular momenta symmetry $SL\pi$ or total angular momentum symmetry $J\pi$ expressed in terms of N-electron target-ion functions χ_i and vector-coupled collision-electron functions θ_i:

$$\Psi_E(e,\text{ion}) = \mathcal{A}\sum_i \chi_i(\text{ion})\theta_i + \sum_j c_j \Phi_j(e,\text{ion}). \quad (1)$$

The χ_i represents a specific state $S_iL_i\pi_i$ or level $J_i\pi_i$ in channel $S_iL_i(J_i)\pi_i\, k_i^2\ell_i(SL\pi \text{ or } J\pi)$, where k_i^2 is the energy of the interacting electron. The second term contains correlation functions Φ_j as products with $N + 1$ bound orbital functions that compensate for the orthogonality conditions between the continuum and the bound orbitals, and represent additional short-range correlation that is often of crucial importance in CC calculations.

*nahar@astronomy.ohio-state.edu

The relativistic N-electron Hamiltonian in the Breit-Pauli (BP) approximation is given by

$$H_{\rm BP} = H_{NR} + H_{\rm mass} + H_{\rm Dar} + H_{so} + \frac{1}{2}\sum_{i\neq j}^{N} g_{ij}(so + so') + g_{ij}(ss') + g_{ij}(css') + g_{ij}(d) + g_{ij}(oo'), \quad (2)$$

where the nonrelativistic Hamiltonian is $H_{NR} = \sum_{i=1}^{N}\{-\nabla_i^2 - \frac{2Z}{r_i} + \sum_{j>i}^{N}\frac{2}{r_{ij}}\}$ and $H_{\rm mass} = -\frac{\alpha^2}{4}\sum_i p_i^4$, $H_{\rm Dar} = -\frac{\alpha^2}{4}\sum_i \nabla^2(\frac{Z}{r_i})$, and $H_{so} = \alpha^2\sum_{i=1}\frac{Z}{r_i^3}l(i)s(i)$ are the relativistic one-body mass-correction, Darwin, and spin-orbit interaction terms, respectively. The rest are two-body interaction terms with notation c for contraction, Dar for Darwin, o for orbit, s for spin, and a prime indicating "other." The first three two-body terms correspond to the full Breit interaction term

$$H_{\rm B} = \sum_{i>j}[g_{ij}(so + so') + g_{ij}(ss')], \quad (3)$$

where the operator form for $g_{ij}(so + so')$ is

$$-\alpha^2\left[\left(\frac{\mathbf{r}_{ij}}{r_{ij}^3}\times\mathbf{p}_i\right)\cdot(\mathbf{s}_i + 2\mathbf{s}_j) + \left(\frac{\mathbf{r}_{ij}}{r_{ij}^3}\times\mathbf{p}_j\right)\cdot(\mathbf{s}_j + 2\mathbf{s}_i)\right],$$

and $g_{ij}(ss')$ denotes

$$2\alpha^2\left[\frac{\mathbf{s}_i\cdot\mathbf{s}_j}{r_{ij}^3} - 3\frac{(\mathbf{s}_i\cdot\mathbf{r}_{ij})(\mathbf{s}_j\cdot\mathbf{r}_{ij})}{r_{ij}^5}\right].$$

Current versions of BPRM codes include the one-body spin-orbit, mass-velocity, and Darwin terms in the interaction Hamiltonian [10]. These codes have now been extended [11] to include the two-body Breit terms given above [Eq. (3)]. In addition, we have also adapted the codes to study features in photoionization into various excited states of the residual ion.

It is necessary to ensure an accurate configuration interaction (CI) expansion for the target ion for electron correlation effects, as well as relativistic effects in the electron-ion system to properly account for fine structure. The O III wave function expansion consists of 19 levels from configurations $1s^22s^22p^2$, $1s^22s2p^3$, and $1s^22s2p3s$. The orbital wave functions of O III were obtained from Breit-Pauli calculations using the program SUPERSTRUCTURE (SS) [12,13]. The set of configurations and Thomas-Fermi orbital parameters were optimized to yield fine structure energies of the ground term $^3P_{0,1,2}$, with and without the two-body terms, and compared with observed values in Table I from the National Institute of Standards and Technology (www.nist.gov). Although, as expected, there is a small effect due to the two-body terms for a light ion such as O III, there is marked improvement in the $^3P_2$ level energy. Details of the more extensive photoionization calculations for recombination of O II will be reported independently.

TABLE I. Fine structure energies for O III ground-state levels.

Level	1-body	2-body	Expt. (NIST)
$2p^2\ ^3P_1$	0.001 015 0	0.000 998 5	0.001 031 4
$2p^2\ ^3P_2$	0.002 988 9	0.002 700 2	0.002 790 1

III. RESULTS AND DISCUSSION

Photoionization cross sections of the ground $2s^22p^{3\,4}S^o$ state of O II in the low-energy region are shown in Fig. 1. Panel (a) presents the featureless and constant $\sigma_{\rm PI}$ in LS coupling [4], and panel (b) presents the total relativistic $\sigma_{\rm PI}$. The next three panels (c)–(e) show partial $\sigma_{\rm PI}$ for photoionization into the fine structure levels $^3P_{0,1,2}$ of the ground state of the residual ion O III. The sharp and narrow resonances at and near the ionization thresholds of $^3P_{0,1}$ of the residual ion in panels (c) and (d) are due to coupling among fine structure channels, not allowed in LS coupling. There are no near-threshold resonances for ionization into the $^3P_2$ level. The total $\sigma_{\rm PI}$ in (b) is the sum of the individual cross sections in (c)–(e), where the background jump at each of the excited ionization thresholds $^3P_1^o$ (d) and $^3P_2^o$ (e) can be seen, in addition to $^3P_0$ (c). The numerous fine structure resonances lying within $E \sim 0.003$ Ry above the first ionization threshold would be important particularly in recombination into O II levels at temperatures 100–1000 K, owing to the maxwellian factor $\exp(-E/kT)$ in recombination rate coefficients. Resonances belong to the Rydberg series $^3P_1^o n\ell$ and $^3P_2^o n\ell$ with calculated quantum defects $\mu_s \approx 0.85, \mu_p \approx 0.55$, and $\mu_d \approx 0.05$; the

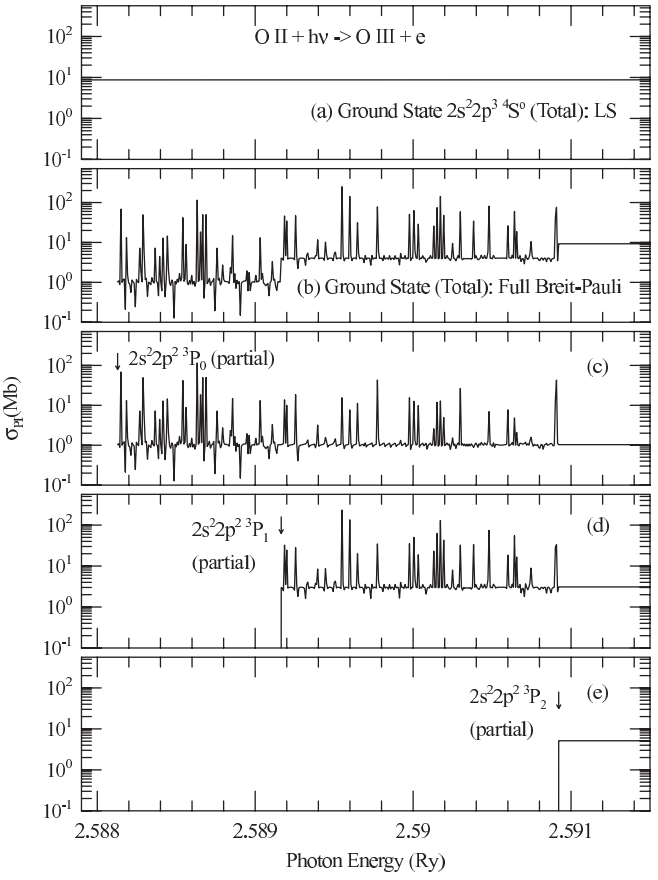

FIG. 1. Near-threshold resonances in photoionization cross sections ($\sigma_{\rm PI}$) of the ground level $2p^{3\,4}S^o_{3/2}$ of O II lying between the O III ground-state fine structure levels: (a) featureless total $\sigma_{\rm PI}$ (LS), (b) total $\sigma_{\rm PI}$ (BPRM), (c)–(e) partial $\sigma_{\rm PI}$ for photoionization into fine structure components $2p^2\ ^3P_{0,1,2}$ of O III, with arrows pointing to the ionization thresholds. The Rydberg series of resonances shown begins with $^3P_1^0 4s, [J = 3/2, 1/2]^o 3\ell$.

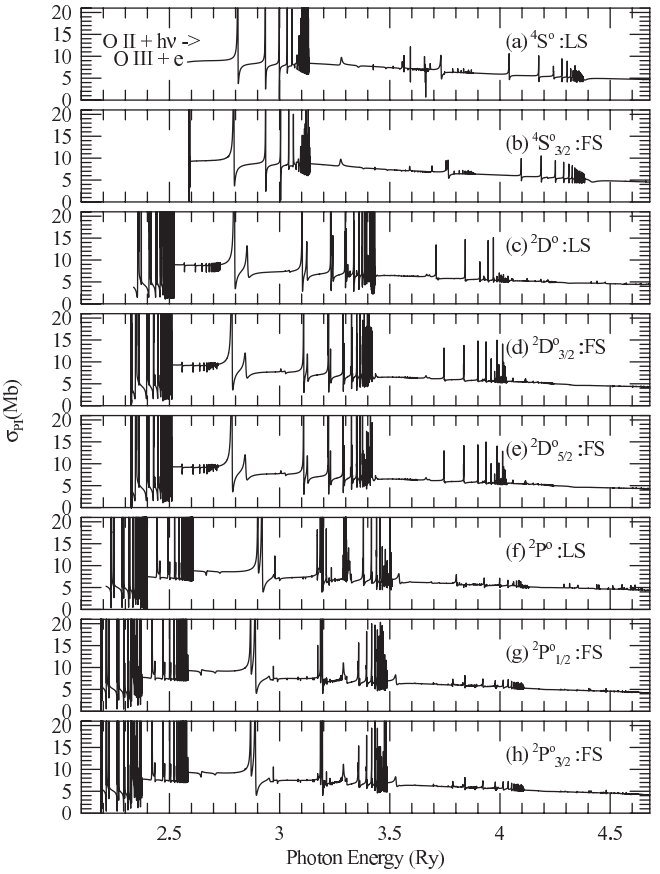

FIG. 2. Comparison of LS and fine structure (FS) photoionization cross sections of ground configuration levels of O II: (a), (b) the ground state $^4S^o$ state (LS) and level $^4S^o_{3/2}$ (FS), (c)–(e) the excited $^2D^o$ state (LS) and $^2D^o_{3/2,5/2}$ (FS) levels, (f)–(h) the excited $^2P^o$ state (LS) and $^2P^o_{1/2,3/2}$ (FS) levels. All fine structure cross sections exhibit more pronounced near-threshold resonances compared with LS ones.

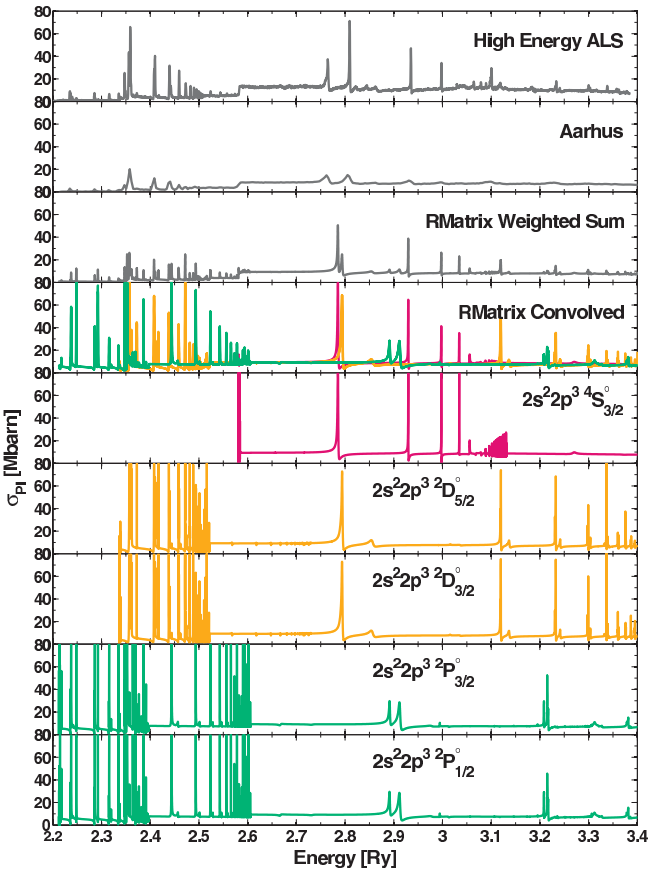

FIG. 3. (Color online) Comparison between experimental results (top two panels, [1,3] and [2]) and theoretical total and convolved photoionization cross sections (3rd panel from top). The lowest five panels present the detailed cross sections and the 4th panel from top represents the cross sections convolved over an experimental beam width of 10 meV.

lowest ones are with $n = 3$ (full identification is in progress). Although the resonances are very narrow, they rise orders of magnitude above the background. Whereas recombinations into excited levels of O II would play a larger role, the resonance enhancement in the ground-state recombination rate coefficient is, for example, a factor of 2–5 at 1000–10 000 K.

Next, we investigate the higher energy region and thresholds for photoionization of not only the ground state $^4S^o_{3/2}$ but also the other excited levels $2s^22p^3(^2D^o_{3/2,5/2},^2P^o_{1/2,3/2})$. Photoionization cross sections of excited levels also show near-threshold structure resonances not found in LS coupling, owing to fine structure splitting. Figure 2 illustrates it through a highly resolved comparison of σ_{PI} in LS coupling and with fine structure. The LS results [5] for σ_{PI} of $^4S^o$,$^2D^o$,and$^2P^o$ states are compared with their fine structure components right below. Figure 2 displays a general comparison of features up to energies above all target thresholds in the 19 CC expansion for O III. As expected for a low-Z ion of a light element, for most of the energy range the overall fine structure effects are not too prominent except for fine structure splitting. The blending of resonant features generally subsumes fine structure splitting in experimental data. However, small shifts in resonance positions due to fine structure components of the core ion levels can be noted. And once again, the most important difference is the resonant structure just above the threshold of each fine structure level.

Owing to the difficulty in resolving these fine structure resonances in a very small energy region, they have not yet been experimentally observed. However, following the work presented in this article, we came across a recent measurement [7] at the ALS facility in Berkeley, capable of very high resolution, that showed similarly narrow but high near-threshold resonances in photoionization of Se II, which has similar electronic configurations as O II; namely, that the ground state is $4p^3\ ^4S^o$ and photoionizes into the $4p^2\ ^2P^o_{0,1,2}$ continua as well. These results imply that if one were to use only the LS photoionization cross sections then two errors would result: (i) the LS ionization threshold of the ^3P term would not account for the shift in energy of the fine structure components $^3P_{0,1,2}$ and (ii) low-energy (temperature) electron-ion recombination via the resonances spanning the fine structure separation would be neglected.

Benchmarking earlier works at the ALS [1,3] showed that the experimental ion beams usually contain not only ions in the ground state but also in low-lying excited metastable levels. Therefore, the measured cross section is the sum of all contributing levels with different populations that are difficult

to ascertain *a priori*. Detailed analysis of resonance structures in level-specific photoionization cross sections is therefore needed to compare with experimental results and to deduce the precise ion-beam composition in terms of excited state distribution(s).

In Fig. 3, the photoionization cross sections $\sigma_{\rm PI}$ from three measurements [1,3] and [2] (top two panels) are compared with the present results (3rd panel from top). Theoretical cross sections of the lowest 5 levels, $^4S^o_{3/2}$, $^2D^o_{5/2,3/2}$, and $^2P^o_{3/2,1/2}$ (panels 5–9 from top) have been convolved with the monochromatic beam width of 10 meV and statistically averaged over the three LS terms (illustrated by the three colors in the panels), to yield results in the 4th panel from the top. Then these are weighted by their known percentage fractions in the beam [1,3], and combined for final comparison in the 3rd panel from top. The overall agreement between the theoretical results and the experimental measurements for almost all resonances is very good. There are a few discernible discrepancies in positions of some resonances. The double feature at ~2.75 eV observed in both experiments appears to be correlated with the series limit of the Rydberg series of resonances on the one hand, and a large resonance complex slightly above. It is also possible that it is formed from another (undetermined) excited state in the experimental beam.

IV. CONCLUSION

The present work is potentially important in both astrophysical applications and benchmarking of high-resolution laboratory experiments. An extensive calculation of recombination rate coefficients into all recombined levels of O II up to $n \leqslant 10$ is in progress to resolve the discrepancy in oxygen abundance determination vis-a-vis the collisionally excited [O III] lines. Highly resolved photoionization cross sections needed for benchmarking are available from the first author.

ACKNOWLEDGMENTS

The computational work was carried out at the Ohio Supercomputer Center in Columbus, Ohio and was partially supported by the US National Science Foundation (Astronomy Division).

[1] A. M. Covington *et al.*, Phys. Rev. Lett. **87**, 243002 (2001).
[2] H. Kjeldsen, B. Kristensen, R. L. Brooks, F. Folkmann, H. Knudsen, and T. Andersen, Astrophys. J. Suppl. Ser. **138**, 219 (2002).
[3] A. Aguilar *et al.*, Astrophys. J. Suppl. **146**, 467 (2003).
[4] Sultana N. Nahar, Phys. Rev. A **58**, 3766 (1998).
[5] Sultana N. Nahar, Phys. Rev. A **69**, 042714 (2004).
[6] R. E. Williams, E. B. Jenkins, J. A. Baldwin, and B. Sharpee, Publ. Astron. Soc. Pac. **115**, 178 (2003).
[7] D. Esteves, N. Sterling, A. L. D. Kilcoyne, R. Bilodeau, E. Red, G. Alna'Washi, R. Phaneuf, B. McLaughlin, C. Ballance, and A. Aguilar, Bulletin of the American Physical Society, 41st Annual Meeting of the APS Division of Atomic, Molecular, and Optical Physics Volume 55, Number 5, Abstract T1.00073 (2010).
[8] Y. G. Tsamis, M. J. Barlow, X.-W. Liu, P. J. Storey, and I. J. Danziger, Mon. Not. R. Astron. Soc. **353**, 953 (2004).
[9] P. J. Storey, Astron. Astrophys. **282**, 999 (1994).
[10] K. A. Berrington, W. B. Eissner, and P. H. Norrington, Comput. Phys. Commun. **92**, 290 (1995).
[11] W. Eissner and G. X. Chen (in preparation).
[12] W. Eissner, M. Jones, and H. Nussbaumer, Comput. Phys. Commun. **8**, 270 (1974).
[13] S. N. Nahar, W. Eissner, G. X. Chen, and A. K. Pradhan, Astron. Astrophys. **408**, 789 (2003).